Volume 13 Number 7 1985 Nucleic Acids Research

# Cleavage within an RNase III site can control mRNA stability and protein synthesis *in vivo*

Nikos Panayotatos and Kim Truong

Department of Molecular Biology, Biogen S.A. 46, route des Acacias, 1227 Geneva, Switzerland

Received 18 January 1985; Revised and Accepted 7 March 1985

ABSTRACT

We report that processing at a cloned bacteriophage T7 RNase III site results in strong stabilization of the mRNA relative to the full-length transcript. In contrast, processing by RNase III of the bacteriophage λ int transcript leads to rapid degradation of the messenger (1-4). It is proposed that the mode of cleavage within the RNase III site determines mRNA stability. Single cleavage leaves part of the phage T7 RNase III site in a folded structure at the generated 3'end and stabilizes the upstream mRNA whereas double cleavage at the λ int site removes the folded structure and accelerates degradation. In addition, the processed transcript is as active a messenger as the unprocessed one and can direct protein synthesis for longer times. This increased efficiency is accompanied by a proportional (3-4 fold) increase in protein levels. In contrast, processing at the λ int site reduces Int synthesis. Thus, processing may either stabilize mRNA and stimulate gene expression or destabilize a messenger and prevent protein synthesis. The end result appears to be determined by the mode of cleavage within the RNase III site.

## INTRODUCTION

Processing by RNase III can alter the stability of mRNA. In the case of the bacteriophage λ int gene, cleavage at the RNase III site leads to faster degradation of the mRNA relative to the unprocessed transcript and, thus, lower levels of int protein synthesis (1-4). On the other hand, bacteriophage T7 mRNAs most of which are processed by RNase III are more stable as a whole than bacterial mRNA (5).

Unlike bacteriophage mRNAs, and bacterial rRNA and tRNA precursors which are extensively processed, very few bacterial mRNAs are believed to be cleaved by RNase III (for a review see reference 6). To investigate this process, we cloned a bacteriophage T7 RNase III site downstream of a constitutively expressed foreign gene, and determined the extent of processing, the stability of the cleavage products and the translation efficiency of the mRNA in vivo.

## MATERIALS AND METHODS

### Construction of pCP62 and pCP63

Construction of these plasmids involved standard genetic engineering techniques used in previous studies (7-10). The origin of the various DNA segments constituting each plasmid as well as their exact sequence coordinates are described in the legend to Figure 1.

### Single-Stranded Restriction Fragment Probes

A 592 base pairs Xba I- Nru I restriction fragment spanning the Sal I site in pCP62 and the equivalent 865 base pairs Xba I-Nru I fragment spanning the RNase III site in pCP63 (Figure 1) were purified by gel electrophoresis. Filling-in with [$^{32}$P]-labelled deoxynucleoside triphosphates followed by strand separation by gel electrophoresis (11) generated anti-sense Xba I-Nru I fragments labelled at the Xba I ends.

### M13 Single-Stranded Probes

The 592 and 865 base pairs Xba I-Nru I fragments from pCP62 and pCP63 were individually cloned at the Sma I site of the M13mp9 vector (12). The size and identity of the inserts were verified by DNA sequencing and restriction mapping. Phages containing the desired strands (designated M13mp9-592 and M13mp9-865) were prepared (12) and stored at 4°C.

The M13mp9-256 probe was prepared by ligating to the filled-in Hind III site of the M13mp9 vector a 256 base pairs Nde I-Afl II restriction fragment (Figure 5) with filled-in ends. In this way, two Hind III sites were generated at the ends of the insert.

To prepare single-stranded DNA probes, E.coli JM101 cultures in 2xTY media were infected with the desired phage at $OD_{590}$=1.0. Thirty minutes later, [$^{32}$P]-orthophosphate (1mCi/10ml) was added and vigorous shaking continued for 5hrs at 37°C. Phage was purified from the supernatants by two polyethyleneglycol precipitations. Single-stranded phage DNA was isolated from the phage by phenol extraction and ethanol precipitation (12). Double-stranded [$^{32}$P]RFI DNA was purified from the cell pellet of the same cultures with a quick-lysis procedure (13). The specific activity was estimated at 1mCi/mg DNA with approximate yields of 1µg RFI DNA and 0.8µg phage DNA per ml culture.

### S1 Protection

Rifampicin (0.2mg/ml) was added to cultures growing exponentially ($OD_{590}$=0.8-1.0) and 5ml samples were transferred in tubes containing 2.5µl diethylpyrocarbonate kept in ice-salt. After centrifugation at 4°C, total RNA was isolated from the cell pellet (14) and resuspended in 50µl $H_2O$.

Hybridization at 65°C, incubation with S1 nuclease at 37°C and electrophoresis on 8% polyacrylamide - 7M urea gels were performed as described (14).

Size Markers

[$^{32}$P]-M13mp9-590 RFI DNA was digested with Hae III and three bands corresponding to fragments 849, 484, and 341 base pairs in length were eluted and used as size markers without prior strand separation. Alternatively, the 865 nt and the 592 nt [$^{32}$P] single-stranded probes were also used as size markers.

Bacterial strains

E.coli MC1061 has been used in previous studies (7). E.coli A0159 rnc$^-$ and A0160 rnc$^+$ which are isogenic except for RNase III were obtained from Ursula Schmeissner. JM101 is the host provided with the M13mp9 vector (New England Biolabs).

Protein labelling

Cultures were grown overnight in L-broth and diluted ten fold with M9 media supplemented with 0.2% glucose, 1mg/liter thiamine and the usual amino acids except cysteine at 10 mg/liter. After 4 hrs at 30°C, the cultures reached mid-exponential phase ($OD_{590}$=1.0). Rifampicin (0.2mg/ml) was added and at various times afterwards [$^{35}$S]-cysteine (0.03mCi/ml). Ten minutes later, L-cysteine (0.4mg/ml) was added and the cultures were chilled quickly in an ice/salt bath. Cells from 1ml culture were processed and analyzed by gel electrophoresis (15).

## RESULTS AND DISCUSION

### Processing of Plasmid-coded mRNA by RNase III

Plasmid pCP62 carries the human interferon $\alpha$5 gene under the control of a constitutive promoter (Figure 1). Plasmid pCP63 was generated by inserting immediately downstream of the 3'-end of the interferon $\alpha$5 gene, 261 base pairs of the DNA sequence surrounding the bacteriophage T7 RNase III site R1.1 (Figure 1).

To test whether mRNA processing occurs at this RNase III site, single-stranded DNA probes complementary to the mRNA between the Xba I and Nru I sites in pCP62 (592 base pairs) and in pCP63 (865 base pairs) were prepared and labelled with $^{32}$P.

Hybridization of total RNA prepared from RNase III$^+$ (rnc$^+$) A0160 cells harbouring pCP63 to the 865 nt probe protected a 498±20 nt fragment from digestion with S1 nuclease (Figure 2, lane 1). The same results were

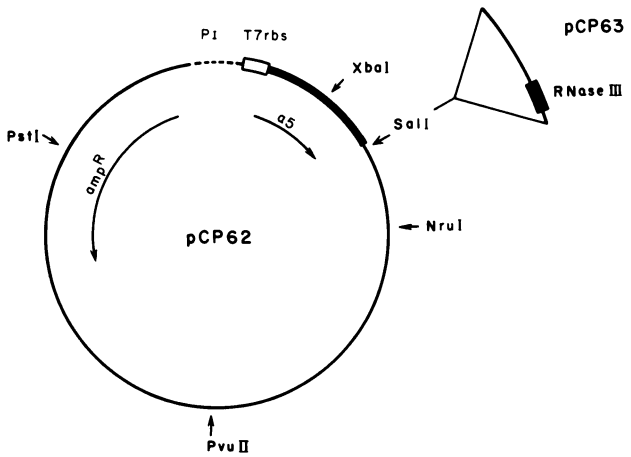


Figure 1. Restriction map of pCP62 and pCP63

Plasmid pCP62 (4,617 base pairs) consists of 263 base pairs (dotted line) of an EcoRI-EcoRI restriction fragment containing the colEI RNAI promoter (8), followed clockwise by a 115 base pairs (open box) EcoRI-Sau3AI restriction fragment from pPI.T7α2 containing the bacteriophage T7 gene 1.1 ribosome binding site (coordinates 5902-6009 of the T7 sequence (20) and the first codon sequence of human leukocyte interferons (8), a 516 base pairs Sau3AI-Taq I fragment containing 501 base pairs (solid bar) coding for the human leukocyte interferon α5 sequence and 15 base pairs (solid line) of the downstream chromosomal sequence from plasmid M51α5 (Ch.Weissmann, personal communication), and, finally, a 3718 base pairs Sal I-EcoRI restriction fragment containing the replicon region and the β-lactamase gene from pBR322 (23).

pCP63 (4,861 base pairs) is identical with pCP62 except for a 261 base pairs HincII-AfI II restriction fragment from pRW307 (10) containing the bacteriophage T7 RNase III site R1.1 (16,20) inserted at the unique Sal I site of pCP62 downstream from the α5 gene (Figure 1).

obtained whether uniformly labelled or 3'end labelled probes were used. The size of the protected fragment corresponded to the product expected if processing occured at the RNase III site (16).

Processing by RNase III should generate a second fragment of uniformly labelled protected probe from the downstream region between the RNase III and the Nru I sites (367 nt). This fragment is barely visible over the heavier background in that region of the gel (Figure 2, lane 1). A weak band was also obtained (Figure 4, lane C) when hybridization was allowed to proceed at a much lower temperature (37°C rather than 65° C) to discount the possibility that the 367 nt fragment did not hybridize as efficiently as the 498 nt fragment due to its smaller size. The weak intensity of the 367 nt fragment suggested that the mRNA sequence downstream from the RNase

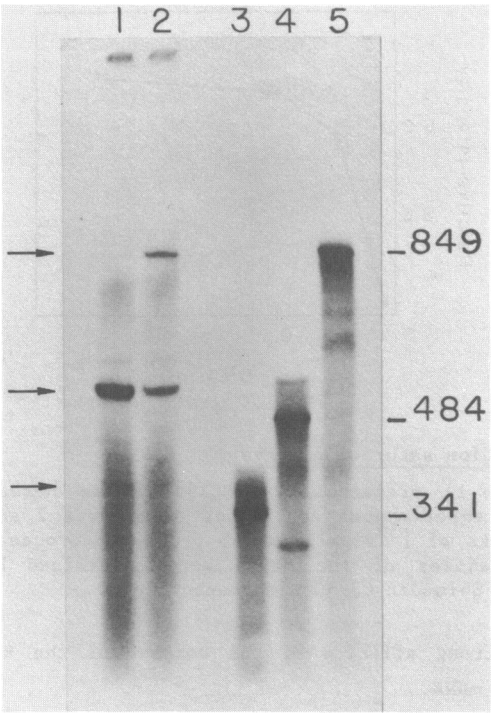


Figure 2. Messenger processing in rnc$^+$ and rnc$^-$ cells

Total RNA was prepared from A0159 rnc$^-$ and A0160 rnc$^+$ cells harboring pCP63, hybridized to the [$^{32}$P]-M13mp9-865 single stranded DNA (0.2 µg) treated with S1 nuclease and electrophoresed on denaturing gels (Methods). On the autoradiograph shown here, Lane 1: RNA (4µl) extracted from rnc$^+$ cells; Lane 2: RNA (4 µl) extracted from rnc$^-$ cells, Lanes 3-5: [$^{32}$P]-Hae III restriction fragments used as markers. The position and the exact length of the single-stranded markers in nucleotides (nt) are shown on the right. The positions of the unprocessed and processed products are indicated by arrows.

III site is degraded faster than the upstream region.

To demonstrate that cleavage of the interferon α5 mRNA at the RNase III site was indeed catalyzed by RNase III total RNA was isolated from an rnc$^-$ isogenic strain (A0159) harbouring pCP63. After hybridization and digestion by S1 nuclease two bands were obtained corresponding to fragments protected by unprocessed (865 nt) and processed (498 nt) mRNA (Figure 2, lane 2). Considering that the stability of the processed mRNA is 3-4 times higher than that of the unprocessed messenger (see below) an estimated 80% of total messenger is not processed in the rnc$^-$ host. The observed processing in these cells may be due to residual levels of RNase III in

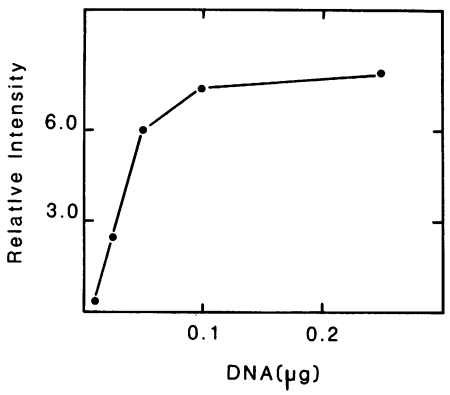


Figure 3. Hybridization saturation curve

Total RNA (4 μ l) prepared from MC1061 cells harboring pCP63 was prepared under the experimental conditions of Figures 2 and 4, hybridized to increasing amounts of [$^{32}$P]-M13mp9-865 probe and processed as in Fig.2. The relative intensities of the bands were determined by scanning the autoradiograph in a Shimadzu CS930 spectrophotometer.

combination with strong affinity of the enzyme for the R1.1 site on the abundant interferon mRNA.

The fact that in rnc$^+$ cells the interferon mRNA is found almost exclusively in the processed form whereas in isogenic rnc$^-$ cells it is found mostly in the unprocessed form indicates that the observed processing is the result of RNase III activity at the homologuous site.

To further demonstrate this point, the precise site of cleavage was determined. Total mRNA was hybridized to the M13mp9-256 probe (Figure 5). The S1-protected fragment was electrophoresed on a DNA sequencing gel along with the four reactions of a known DNA sequence as a marker (data not shown). Three bands corresponding to DNA fragments 211, 212 and 213 nt long were obtained. The size of these fragments corresponds to the size (212 nt) expected if processing by RNase III occurs at the reported site (16). Therefore, the protected fragments must indeed be the result of precise mRNA processing by RNase III at the R1.1 site.

A major difficulty in studying mRNA cleavage is that putative "processing" sites prove occasionally to be "leaky" transcriptional terminators. This does not seem to be the case here. The T7 RNase III 1.1 site under study is a well characterized processing site both in vivo and in vitro (16,17) which does not act as a rho-dependent terminator (18). The observed reduction in the extent of processing in the rnc$^-$ strain as well

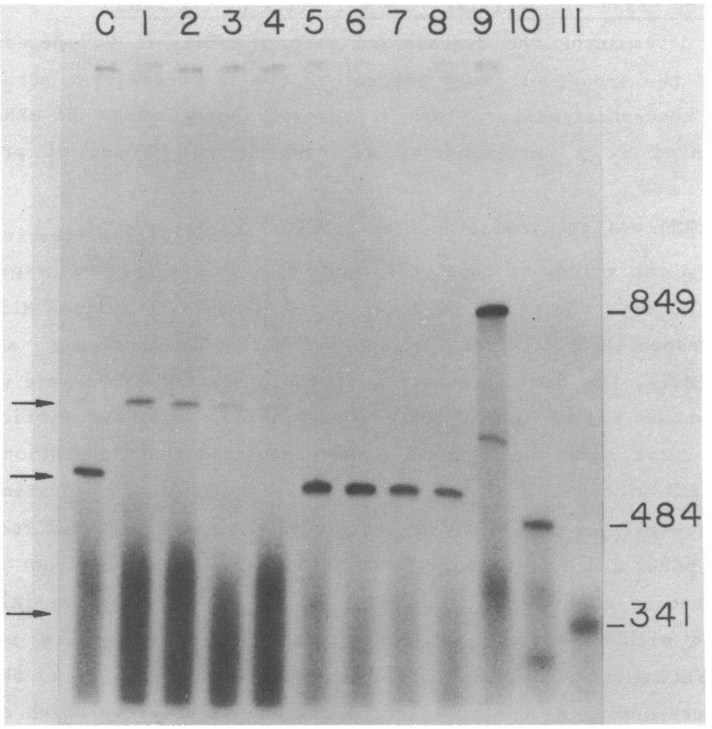


Figure 4. Decay of full-length and processed mRNAs

Transcription initiation was blocked by the addition of rifampicin to exponentially growing cultures. Total RNA prepared at the indicated times from MC1061 cells harboring pCP62 was hybridized to the [$^{32}$P]-M13mp9-592 probe (lanes 1-4) and total RNA prepared from MC1061 cells harboring pCP63 was hybridized to the [$^{32}$P]-M13mp9-865 probe (lanes 5-8). The size markers described in Fig.2 were loaded on lanes 9-11. A sample hybridized at 37°C was loaded on lane C. An autoradiograph of samples removed at 0min (lanes 1,5); 2min (lanes 2,6); 5min (lanes 3,7); and 8min (lanes 4,8) is shown here. The positions of the unprocessed and processed products are indicated by arrows.

as the fact that the cleavage site of the interferon α5 mRNA coincides with that of T7 mRNA processed in vivo strongly argue that the protected 498 nt and 367 nt fragments are produced after processing of the mRNA by RNase III. The differential intensities of the bands corresponding to the protected segments of mRNA upstream and downstream of the RNase III site must, therefore, be attributed to differential stability of the cleavage products.

Processing by RNase III Increases the Half-life of the mRNA

Before determining the degradation rate of mRNA, it was necessary to ensure that the amount of probe was not merely in excess, but actually at saturating concentrations, so that a decrease in the amount of mRNA would be accompanied by a corresponding decrease in the amount of protected probe.

Total mRNA was prepared from E.coli MC1061 rnc+ cells harbouring pCP62 or pCP63 and the volume of total RNA (4µl) used in the previous experiments was incubated with increasing amounts of the M13mp9-592 and the M13mp9-865 probes, respectively. After digestion with S1 nuclease and gel electrophoresis, the band intensities of the protected probe were measured and plotted as a function of DNA concentration. From the hybridization saturation curve shown in Figure 3 it was concluded that incubation of 4µl of total mRNA with 0.2µg of the M13mp9-865 probe ensured saturating probe conditions. Similar curves were obtained with total RNA prepared from cells harbouring pCP62 and hybridized with the M13mp9-592 probe (data not shown).

To determine the half-life of mRNA in vivo, transcription initiation was blocked with rifampicin and S1-protection experiments were performed under saturating concentrations of probe. The results (Figure 4) show that a band corresponding to the full length of the 592 nt probe which does not contain the RNAse III site is protected from S1 nuclease. The intensity of this band begins to decrease immediately after the addition of rifampicin and less than 20% remains 5min later. In contrast, the intensity of the 498 nt probe generated from the sequence upstream of the RNase III site appears to increase 2min after the addition of rifampicin and 90% of the probe is still protected at 5min. (The initial increase in intensity has been observed with other long-lived mRNAs (19)). Semi-logarithmic plots of band intensity versus time showed that the unprocessed mRNA decays with a half-life of 2½min, whereas the mRNA fragment generated by RNase III decays with a half-life of approximately 9min. Thus, processing by RNase III resulted in a 3-4 fold increase in the stability of the mRNA segment upstream from the cleavage site.

However, only the upstream fragment of mRNA became more stable. The downstream part appeared to be degraded with a half-life similar to that of the unprocessed trancript, although the weak intensity of the corresponding band did not permit accurate measurements. Since this mRNA cleavage product and the unprocessed transcript terminate at the same 3'ends their half-lives would be expected to be the same, if mRNA degradation occurred

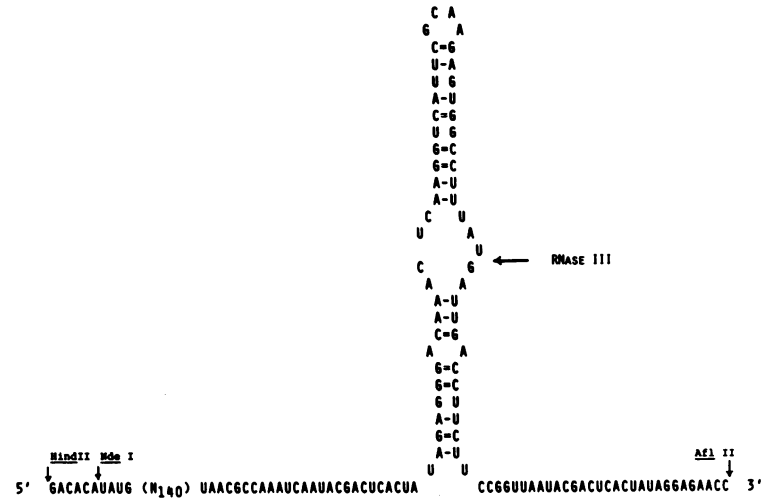


Figure 5. RNA Sequence around the RNase III R1.1 site

The sequence of the transcript through the 261 base pairs HindII - Afl II restriction fragment inserted in pCP63 is drawn in a potential hairpin structure (20). The position of a few restriction sites and the point of cleavage by RNase III are also shown.

primarily exonucleolytically from the 3'end.

By analogy, the unprocessed mRNA and the processed fragment upstream from the RNase III site share the same 5'ends and, accordingly, the increased stability of the latter should be attributed to increased resistance to exonucleolytic degradation from the 3'end. Evidence for 3'-to-5' directionality in mRNA decay was obtained in a recent study (19).

Geometry of Cleavage Determines Stability

Processing at the bacteriophage T7 RNase III 1.1 site generates an upstream mRNA fragment which maintains at its 3'end a portion of the hairpin structure of the RNase III site, and a downstream fragment whose newly generated 5'end sequence loses the potential of being involved in a double stranded structure. This feature is a consequence of the particular location of the cleavage point relative to the loop of the proposed secondary structure for the R1.1 site (Figure 5).

Folding of the 3'end in a secondary structure is believed to protect the RNA from 3'-to-5' exonucleolytic degradation. Therefore, the observed 3-4 fold increase in stability of the processed upstream fragment may indeed be due to the fact that its 3'end is protected. In this case,

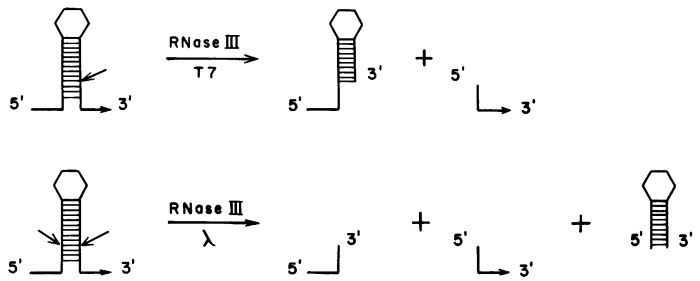


Figure 6. Single and Double Cleavage by RNase III

The hairpin structures represent the secondary structure of the mRNA before and after processing. The R1.1 site studied here is cleaved once and the upstream product can maintain a folded structure at its 3'end which (presumably) protects the messenger from degradation. All RNase III sites of bacteriophage T7 share this mode of cleavage and the processed transcripts are relatively stable. In contrast, the bacteriophage λ *int* gene processing site is cleaved twice and the upstream product which can not maintain a folded structure at its 3'end becomes labile. The small RNA product of double cleavage shown in a hairpin structure is a stable species.

processing at other RNase III sites sharing the same geometry of cleavage should also result in more stable processed mRNAs.

This argument (20) has been advanced to explain why bacteriophage T7 mRNAs are much more stable ($t\frac{1}{2}$=6-20min) than bacterial *trp* mRNAs ($t\frac{1}{2}$=80sec) (5). Inspection of the proposed secondary structures and cleavage points of all ten T7 RNase III sites shows that processed T7 mRNAs may contain their 3'termini in hairpin structures similar to the R1.1 site (20). Our finding that processing at the R1.1 site leads to mRNA stabilization provides evidence consistent with this hypothesis.

In contrast to the increased mRNA stability after cleavage at the T7 R1.1 site, processing at the bacteriophage lambda *int* site results in much faster degradation of the processed mRNA relative to the intact transcript (2-4). Unlike the T7 RNase III sites, however, cleavage at the λ *int* site occurs at both ends of the stem-and-loop structure. Such cleavage generates an upstream mRNA fragment which does not contain part of the folded structure of the RNase III site (Figure 6). The fact that this processed mRNA is rapidly degraded is also consistent with the hypothesis that processing leads to RNA stability only if part of the folded structure remains at the 3'end. Perhaps the RNase III enzyme remains bound at the 3'end providing additional protection from other nucleases.

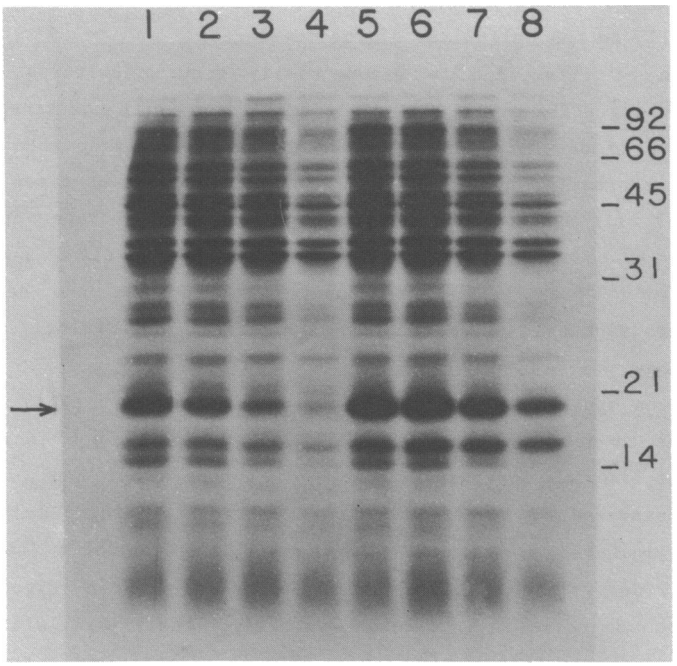


Figure 7. Protein Synthesis after Transcription Arrest

Rifampicin was added to E.coli MC1061 cells bearing pCP62 or pCP63 to block transcription initiation. At the indicated times [$^{35}$S]-cysteine was added for 10min, and samples were analyzed by gel electrophoresis and autoradiography. Lanes 1-4: pCP62/MC1061 cells labelled at 0, 3, 6 and 10min after the addition of rifampicin. Lanes 5-8: pCP63/MC1061 cells labelled in parallel.

## Processed mRNA is Active Messenger in vivo

The basis of the retroregulation model for the $\lambda$ int gene is that processing by RNase III causes rapid mRNA degradation (1). In that case, the RNase III enzyme acts as a negative regulator of gene expression. On the other hand, in the case of the T7 RNase III sites where the processed mRNAs become more stable, processing by RNase III might have a positive effec on gene expression if the cleaved transcripts were active mRNAs and not inactive degradation intermediates.

Processing at the R1.1 site in pCP63 was found to increase the half-life of the human interferon $\alpha$5 mRNA 3-4 fold relative to the unprocessed transcript. If the processed transcript were as efficient a messenger as the unprocessed one then, after blocking mRNA synthesis with rifampicin,

protein synthesis catalyzed by the decaying mRNA should be prolonged proportionally to the half-lives of the messengers.

Addition of rifampicin to exponentially growing cultures of MC1061 cells harbouring pCP62 or pCP63 leads to mRNA decay with the kinetics shown in Figure 4. To determine the efficiency of the surviving mRNA molecules for protein synthesis, [$^{35}$S]-cysteine was added at various times after the addition of rifampicin and was allowed to incorporate into newly synthesized protein for 10min. Visualization of labelled proteins by autoradiography after gel electrophoresis showed that the decrease of interferon $\alpha$5 synthesis after transcription arrest is strikingly similar to the mRNA decay.

Interferon synthesis catalyzed by unprocessed mRNA in cells harbouring pCP62 begins to decrease 2min after the addition of rifampicin and decays with a half-life of approximately 2½min. On the other hand, interferon synthesis catalyzed by processed mRNA in cells harbouring pCP63 shows the same small increase as the mRNA 2min after addition of rifampicin and subsequently decays with a half-life of approximately 9min (Figure 7). The fact that the decrease in interferon synthesis closely parallels the decay of mRNA demonstrates that the processed mRNA is as efficient a template for protein synthesis as the unprocessed one.

In addition, since the processed mRNA can function as active messenger 3-4 times longer, the levels of human interferon $\alpha$5 protein are also increased. This increase can be observed in Figure 7 by comparing the band intensities of $\alpha$ 5 interferon in cells harbouring pCP62 and pCP63. Moreover, measurements of interferon $\alpha$5 activity in cells harbouring pCP63 revealed 3-4 times higher levels of active interferon than in cells harbouring pCP62 (data not shown). These results demonstrate that RNase III acts, in this case, as a positive modulator of gene expression.

Mechanism of mRNa Stabilization by Processing

The overall effect of RNase III processing on mRNA stability also depends on factors other than the potential to maintain part of the RNase III site in a hairpin structure at the 3'end. In the case of transcripts terminating several thousand base pairs beyond the RNase III site, processing might on one hand stabilize the upstream product and on the other accelerate its degradation by bringing the 3'end of the transcript much closer to the gene. Since messenger stabilization is measured relative to the unprocessed transcript, its magnitude would depend on the resistance to 3'-to-5' exonucleolytic degradation of the 3'termini of the unprocessed

transcripts. In the case of labile unprocessed transcripts the net effect of processing by RNase III on mRNA stability might be quite substantial.

It should also be noted that the protected single-stranded probe fragments were visible on the polyacrylamide gels after staining with ethidium bromide. This observation (which may eliminate the use of labelled probe in future experiments) suggested that the intracellular levels of interferon mRNA were quite high. If a visible band roughly represents 10ng of the 498 nt fragment (20% of total at saturating probe concentrations) then the number of $\alpha$5 interferon mRNA molecules per cell is calculated at 200.

Despite the fact that the interferon mRNA levels are approaching those of the most abundant bacterial mRNA (21), processing by RNase III was found to be complete. This result suggested that RNase III is present in the cell in large excess. Therefore, small variations in its levels are not likely to determine the extent of processing. Instead, the key element to processing appears to be the presence of an RNase III site downstream from the gene, and the main determinant of the fate of the processed transcript appears to be the location of the cleavage point within that site. Between the level of mRNA lability conferred by $\lambda$ *int*-like double cleavage and the stabilization provided by T7-like single cleavage, the half-life of the messenger can be altered by more than an order of magnitude. Within this range, the affinity of the particular RNase III site for the enzyme may determine the precise degree of messenger stability.

Bacterial mRNAs are not normally processed by RNase III. However, the evidence presented here suggests that any plasmid-coded mRNA would be efficiently processed if it contained an RNase III site. The absence of such sites may account for the lack of processing of bacterial mRNA as opposed to bacteriophage mRNAs and precursor rRNAs and tRNAs. Alternatively, however, RNase III sites may be present in bacterial mRNAs but may not be accessible to the enzyme. In this case, the fact that the $\alpha$5 interferon mRNA is efficiently processed would imply that the cell can somehow distinguish plasmid-coded mRNA from genomic mRNA. The observation that plasmid DNA appears to resemble phage rather than bacterial DNA in its resistance to nucleolytic attack *in vivo* (22) might be a related phenomenon.

ACKNOWLEDGMENTS

We thank our Biogen colleagues, Dominique Semon for the M13 cloning and

the sequencing gel electrophoresis, Albert Schmitz for the S1 mapping protocol, Philip Whitehead for the Afl II enzyme, and Nadine Huber for expert typing.

REFERENCES

1. Schmeissner, U., McKenney, K., Rosenberg, M. and Court, D. (1984). J.molec.Biol. 176, 39-53.
2. Lozeron, H.A., Anevski, P.J., and Apirion, D. (1977). J.molec.Biol. 109, 359-365.
3. Lozeron, H.A., Dahlberg, J.E., and Szybalski, W. (1976). Virology, 71, 262-277 (1976).
4. Guarneros, G., Montanez, C., Hernandez, T. and Court, D. (1982). Proc. Natl.Acad.Sci.USA 79, 238-242.
5. Marrs, B.L. and Yanofsky, C. (1971). Nature New Biol. 234, 168-170.
6. Gegenheimer, P. and Apirion, D. (1981). Microbiol.Rev. 45, 502-541.
7. Panayotatos, N. (1984). Nucleic Acids Res. 12, 2641-2648.
8. Panayotatos, N., Fontaine, A., and Truong, K. (1983). J. Cellular Biochem. Suppl 7B, 109.
9. Panayotatos, N. and Truong, K. (1981). Nucleic Acids Res. 9, 5679-5688.
10. Panayotatos, N. and Wells, R.D. (1979). J. biol. Chem. 254, 5555-5561.
11. Maxam, A.M. and Gilbert, W. (1980). Methods Enzymol. 65, 499-559.
12. Messing, J., and Vieira, J. (1982). Gene, 19, 269-276.
13. Klein, R.D., Selsing, E., and Wells, R.D. (1980). Plasmid, 3, 88-91.
14. Brosius, J., Cate, R., and Perlmutter, A.P. (1982). Proc. Natl. Acad. Sci. USA 257, 9205-9210.
15. Laemmli, U.K. (1970). Nature, 227, 680-685.
16. Robertson, H.D., Dickson, E., and Dunn, J.J. (1977). Proc. Natl. Acad. Sci. USA 74, 822-826.
17. Rosenberg, M., Kramer, R.A. and Steitz, J.A. (1975). In "Processing of RNA" (J.J.Dunn, ed.) pp 277-285. Brookhaven National Laboratory, Upton, N.Y.
18. Dunn, J.J. and Studier, F.W. (1973). Proc.Natl.Acad.Sci.USA 70, 1559-1563.
19. Von Gabain, A., Belasko, J.G., Schottel, J.L., Chang, A.C.Y., and Cohen, S.N. (1983). Proc. Natl. Acad. Sci. USA 80, 653-657.
20. Dunn, J.J. and Studier, F.W. (1983). J. molec. Biol. 166, 477-535.
21. Hirashima, A., Wang, S. and Inouye, M. (1974). Proc.Natl.Acad.Sci.USA 71, 4149-4153.
22. Panayotatos, N. and Fontaine, A. (1985). J.Biol.Chem.(in press).
23. Sutcliffe, J.G. (1979). Cold Spring Harbor Symp. Quant. Biol. 43, 77-90.